https://doi.org/10.59893/abud.25(1).009
Acta Biol. Univ. Daugavp. 25(1) 2025
ISSN 1407 - 8953

LAND USE AND LAND COVER CHANGE IMPACTS ON GROUNDWATER AVAILABILITY PROJECTIONS: A CASE STUDY OF THE TALOMO-LIPADAS WATERSHED

Danieca Louise E. Talaid*, Assel Jeunne C. Vitor, Renato F. Lemente Jr., Jason Ben R. Paragamac

Talaid D.L.E., Vitor A.J.C., Lemente Jr R.F., Paragamac J.B.R. 2025. Land use land cover change impacts on groundwater availability projections: a case study of Talomo-Lipadas watershed. *Acta Biol. Univ. Daugavp., 2025(1):139-161.*

Abstract
The rate of land use and land cover (LULC) change is critical in determining the sustainability of groundwater resources, often linked to rapid urbanization and population growth. This study examines spatio-temporal LULC changes in the Talomo-Lipadas watershed by analyzing geomorphological and hydrological parameters to predict groundwater availability, hypothesized to be influenced by shifting LULC and rainfall patterns. Using Geographic Information System (GIS), statistical models, the analysis revealed that the watershed is predominantly rolling to moderately steep, with slopes ranging from 15-30% and elevation of <530 above mean sea level, which accounts 89.79% or 35,349.90 ha. The area has an average population density of 15/km2 and is dominated by clay-loam soil type. LULC trends presented that built-up areas (BUA) peaked in 2019 at 1.42% and forest areas had the highest decline in 2020 at -4.08%, agricultural land decreased in 2021 by -3.97%, and shrubland declined by -0.40% in 2022. Precipitation patters showed consistent levels from 2018 to 2022 but declined from 2021 to 2023, with the lowest rainfall of over 300 mm in 2023. Groundwater availability projection using linear, exponential, cubic, and support vector regression model indicate a downward trend, correlating with the changes in LULC and precipitation. Regression analysis confirmed a strong positive correlation between the variables, identifying that all models were reliable predictors. These findings call out the action to integrate LULC dynamics and rainfall trends in groundwater management and urban planning strategies.

Keywords: Land use and land cover, groundwater availability, support vector regression, and watershed management.

*Corresponding author: *Danieca Louise E. Talaid. Environmental Studies Department, University of Mindanao, 8000, Davao City, Philippines. E-mail: d.talaid.517511@umindanao.edu.ph.*

Assel Jeunne C. Vitor. Environmental Studies Department, University of Mindanao, 8000, Davao City, Philippines

Renato F. Lemente Jr. Environmental Studies Department, University of Mindanao, 8000, Davao City, Philippines

Jason Ben R. Paragamac. College of Environmental Studies, Marinduque State University, Professional Schools, University of Mindanao, 8000, Davao City, Philippines

INTRODUCTION

Planned or unplanned urbanization is influential in landscape fragmentation. Groundwater is the prime natural resource on Earth and not only supports types of life forms existing on Earth but also helps in the growth of human civilization (Simlandy 2015). The groundwater recharge has been declining for years and will continue to do so in the absence of corrective measures. For instance, the value of groundwater recharge provided by a watershed depends on both the quality of g2roundwater extraction and the amount of watershed conservation (Roumasset & Wada 2013). This requires solving for the dynamic management of two interacting resources. Consequently, a watershed provides services such as nutrient cycling, carbon storage, soil formation, erosion control, flood control, water storage, filtration, timber, and recreation (Aldridge et al. 2017). However, rapid urbanization and intensive agricultural development create irreversible impacts on watersheds, affecting the quantity and quality. It involves the development and conversion of land into different types of infrastructure, which causes natural watershed conditions by altering its terrain, vegetation, and various hydrologic and geomorphic impacts (European Environment Agency 2014). Increased water demand in the cities poses serious stresses to watershed ecosystem function, structure, and services, for example, water quality degradation (Sun & Caldwell 2015) leads to alteration leads to a reduction in the soil water infiltration capacity and groundwater recharge, thereby impacting the hydrological processes within the watershed (Sertel et al. 2019). Currently, this is the most important and main water source for Davao City as it has aquifers that provide 99% of the city's demand for water (Branzuela 2015). Predicting groundwater associated with LULC is limited to no data, particularly in the Talomo-Lipadas watershed. It has also been observed that the published successful studies have only focused on the existing LULC data and water supply within international countries (Banjara et al. 2024), and there are no existing studies evaluating the status of the LULC change and hydrological changes in Talomo-Lipadas yet. The general objective of the study is to assess how LULC potentially influenced the groundwater availability of the Talomo-Lipadas watersheds. Specifically, this aimed to (1) analyzed slope ranges, elevation ranges, population density, distance to river, distance to road network, LULC changes 2018-2023, (2) rainfall distribution 2018-2023, (3) explore different statistical models in predicting groundwater availability in Talomo-Lipadas watershed.

MATERIAL AND METHODS

The research design in the study is descriptive and quantitative non-experimental. This involves utilization of Geographic Information System (GIS) to spatially map changes of LULC and its potential influences on groundwater resources in Talomo Lipadas Watershed. Data collection involves the acquisition of satellite imagery from ESRI Sentinel-2 land cover explorer and Landsat data from 2018-2023 to quantify LULC patterns. Shapefiles containing data of Talomo-Lipadas watershed were requested and obtained from Department of Environment and Natural Resources- Forest Management Bureau (DENR-FMB). The acquired satellite images undergo reclassification processes and categorize land use land cover data on various groups. In generating LULC maps, raster data from Esri Sentinel-2 Land Cover Explorer (ArcGIS Living Atlas of the World n.d.) were imported in QGIS. The raw raster data were used to make LULC maps from 2018-2023 which produced to six (6) Landsat scenes. In terms of

predictor variables, it used utilized river network. The river networks were determined using the SWAT+ (Soil and Water Assessment Tool) interface in QGIS. The SWAT+ (Bieger et al. 2016) tool is a supplement is a technique for assessing soil, water, and basin management (Montoya 2017). The roadway networks were done in QGIS using OSM (OpenStreetMap) Downloader Plugin (OpenStreetMap Contributors 2015). The generated roadway networks were used to determine the route of urban centers closing in the watershed. In terms of its distance to rivers, it used the Euclidean distances incorporated in QGIS. For population density, the spatial distribution of the population in all barangays under Talomo-Lipadas watershed for the year 2020 was obtained from PhilAtlas public website (PhilAtlas n.d.). The spatial distribution and mapping were performed using QGIS 3.28.15. The global soil map shapefile and the mdb file that contains the information about soil types present in each country were sourced from Food and Agricultural Organization of the United Nations Soils Portal (Fao/UNESCO soil map of the world | Fao soils Portal | Food and agriculture organization of the United Nations 1961). The distribution of soil types and its area were characterized using QGIS 3.28.15. For elevation, the DEM data were obtained from SRTM DEM Downloader (NASA Shuttle Radar Topography Mission (SRTM). 2013) of QGIS 3.28.15 with a resolution of 30x30 meters. The slope map creation is done through using the analysis slope tool option in QGIS. A six-year rainfall data from PAGASA to generate rainfall map distribution through Inverse Distance Weighting (IDW) Interpolation. In addition, the initial tabulated data from 1977 to 2017 on the water availability profile and the relevant parameters obtained from the study conducted by Espina (2022) titled, The Water-Energy Nexus: Exploring Options for Davao's Future which were also sourced from Davao City Water District (DCWD). In assessing the Annual Rate of Change (ARC), the data on land classifications was collected to determine annual variability. The ARC analysis is carried out to quantify differences in LULC between the initial and final years. The ARC was calculated using the following formula (Yuan et al. 2024):

$$ARC(\%) = \frac{F_y - I_y}{I_y \cdot t} \times 100$$

where:

Fy = Final value of the variable in year y;
Iy = Initial value of the variable in year y;
t = Time period in years.

Due to the limited data available from the DWCD, predictions were made to fill in the gap between the latest available data, which was from 2017 up to 2023, using linear, exponential, and cubic statistical models.

Linear model is:

$$y=mx+b$$

where:

y = Predicted value;
m = Slope of the line;
X = Independent variable (year);
B = Intercept.

Exponential model:

$$y=a \cdot e^{bx}$$

where:

y= Predicted value;
a= Initial value;
e= Euler's number (approximately 2.718);
B = Growth rate;
x= Independent variable (year).

Cubic Model:

y=ax3+bx2+cx+dy = ax^3 + bx^2 + cx + dy=ax3+bx2+cx+d

where:

Y = Predicted value;
A, b, c = Coefficients of the cubic equation;
D = Intercept;
x = Independent variable (year).

These three models are crucial in determining which approach is best suited to forecasting future water demand. If the R squared of the linear model for the actual data set is 0.90 to 0.99, then the model set resembles the actual set. A multiple regression analysis is used to determine the relationship of the LULC changes with the forecasted groundwater availability. The general equation of multiple regression is:

$$y=\beta0 +\beta1\ x1 +\beta2\ x2 +\cdots+\beta n\ xn +\varepsilon$$

where:

Y = Dependent variable (groundwater availability);
β0 = Intercept;
β1, β2 βn = Coefficients for each independent variable;
x1, x2, xn = Independent variables (e.g., land use categories, rainfall, etc);
ε= Error term.

Aside from these three models, Support Vector Regression (SVR) was used to analyze and project values as it is one of the powerful machine learning methods for groundwater level projection. Its capacity to handle complex, and non-linear relationships (Satapathy & Sahoo 2023) makes it suitable to achieve the objectives of this study (). This approach has been performed by multiple studies including the study of Mukherjee and Ramachandran (2018), where they generated prediction for unevenly spaced time series data of groundwater levels (GWR) in India. In this research, this method is implemented using R studio version 4.4.3 through "e1071" package, which provides svm() functions that supports both Support Vector Machines (SVM) and SVR (Meyer et al. 2024). The svm() function was utilized where groundwater is a function of the chosen predictor variables such as the rainfall and built-up land percentages. Also, predict() function was employed to present predictions for missing groundwater values after fitting the model to the parameters data (Kowalczyk 2014).

In Coefficient of Determination, R^2 is a measure of goodness of fit and is used as the basis of precision in predictions for the general linear model (Barrett 2012). This approach can be viewed as a measure of proportion of the sum of the squares of deviation. Several studies have also used this type of analysis to determine the correlation and how the models involved would be suitable for the given data set. Researchers used Microsoft Excel to carry out this method. This can be written as:

$$R^2 = 1 – (RSS/TSS)$$

where:

R^2 = Coefficient of Determination;
RSS = Residuals sum of squares;
TSS = Total sum of squares.

The study area is in located in Davao City, Philippines. Specifically, the Talomo-Lipadas Watershed. The Talomo-Lipadas Watershed comprises approximately 39,595.76 hectares and it's divided into two main sub-watersheds – the Talomo watershed and Lipadas watershed. The Talomo-Lipadas Watershed is mostly made up of agricultural, grassland, shrublands, and forest resources (Ibañez et al. 2012). Although Talomo-Lipadas Watershed covers only 12% of the city's land area, it is currently the most important water source for Davao City with its aquifers serving 99% of the city's demand for water (Ibañez et al. 2012), as the watershed of Tamugan River is reportedly to have the highest quality of water which is Class AA (Espina 2022). Given that, it is essential to study this watershed in the present because it is a significant source of water for the city in the future since it is the only sub-watershed that easily meets the requirement for quality water for national drinking and previous studies found that the remaining primary growth forests in the watershed support a rich and endemic community of flora and animals.

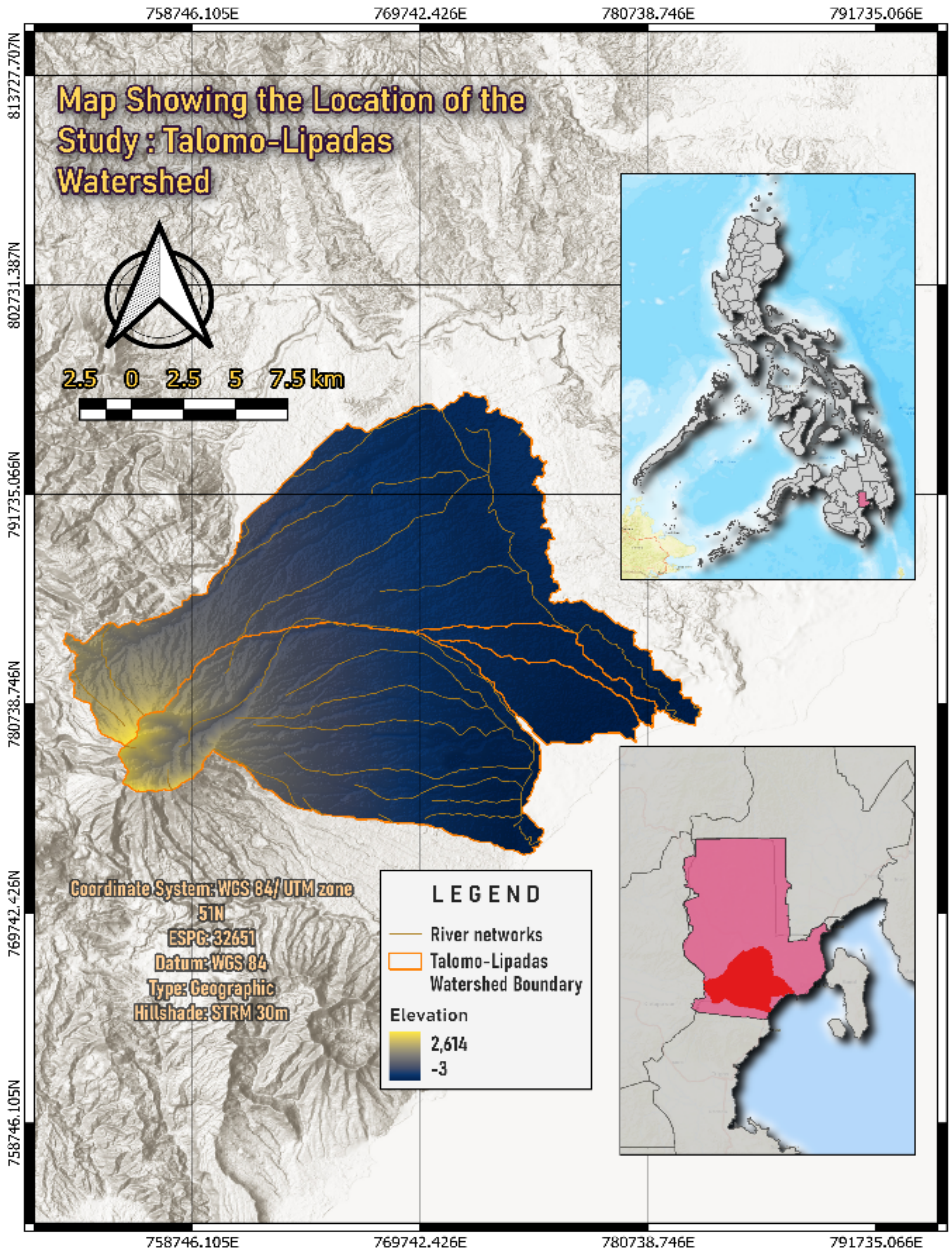

Figure 1. Maps showing the location of the Talomo-Lipadas Watershed.

RESULTS AND DISCUSSION

Characteristics of Talomo-Lipadas Watershed

Presented in Table 1 and Figure 1 (a) is the slope ranges and slope map of Talomo-Lipadas watershed. Data have showed that the study area is classified rolling to moderately steep comprises the 85.5% or a total land area of 33,651.97 ha with a slope range of 15-30%, followed by steep with 10.01% which accounts the 3,959.05 ha with slope percentage of 30-45% and the least is very

steep with slope percentage of 50% and above which covers the 5.01% or a total land area of 1,984.74 ha. This indicates that the steeper the slope, the greater the chances that it will facilitate the flow resulting in large amount of water to the transport of the soil. Thus, the increment of erosion on steep slopes is the result of an increase of surface runoff and which influences the decline of infiltration (Morbidelli et al. 2018).

Table 1. Slope Gradient of Talomo-Lipadas Watershed.

Slope Category	Area (ha.)	Area in %
Rolling to Moderately steep (15-30%)	33651.97	85.0
Steep (30-45%)	3959.05	10.0
Very steep (50% above)	1984.75	5.01
Total	39595.77	100%

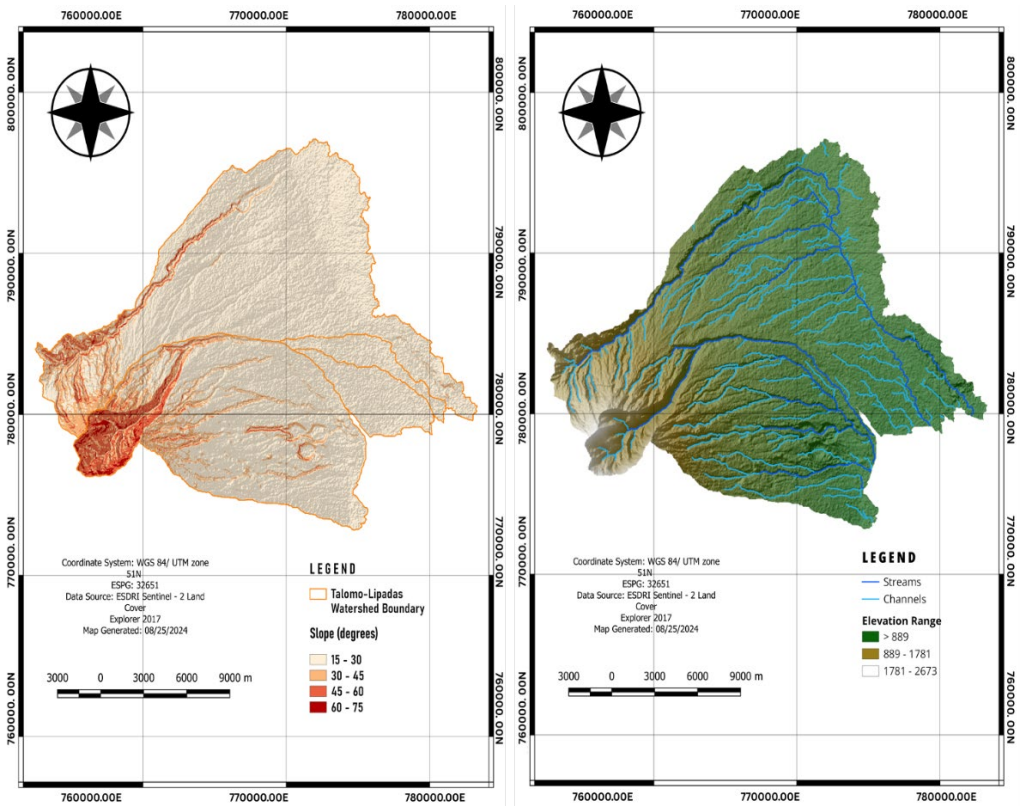

Figure 2. Maps showing the slope ranges and elevation ranges of Talomo-Lipadas Watershed.

In terms of elevation ranges, majority of the study area fall under an elevation category of <530 mean above sea level which accounts the 35,549.90 ha, followed by 1,604-2,138 masl which covers the 10.15% of the total land area and the least falls under the 2,139-2,673 masl which accounts .05% of the total land area of Talomo-Lipadas watershed. Higher elevations potentially serve as a critical source of water and lower elevations support human activities. Typically, higher elevations warm more quickly and receive greater rainfall, while lower areas experience less rainfall, with the most significant increase occurring in lowland regions, making the terrain more subdued (Pepin et al. 2022). Groundwater flow is

inherently complex, forming local, intermediate, and regional flow systems influenced by various factors. Topographic terrain plays a crucial role in shaping these flow systems (Henriksen 1995, Grinevskii 2014, Dai et al. 2021). Talomo River reflects the highest elevation in the said watershed, while nearby barangays were considered as the lowest elevation, ranging from 0 to 1,000 km. Although the area is small, it contributes to the watershed retention. Furthermore, about 21.97 ha or 10.15% of the watershed lies within high elevation ranges, which is characterized by forest cover, less human habitation, a more protected environment, and includes the steepest and most elevated parts of the watershed.

Table 2. Elevation ranges of Talomo-Lipadas Watershed.

Elevation Category (masl.)	Area (ha.)	Area in %
<530	35549.90	89.79
1604-2138	4018.69	10.15
2139-2673	21.97	0.05
Total	39595.77	100%

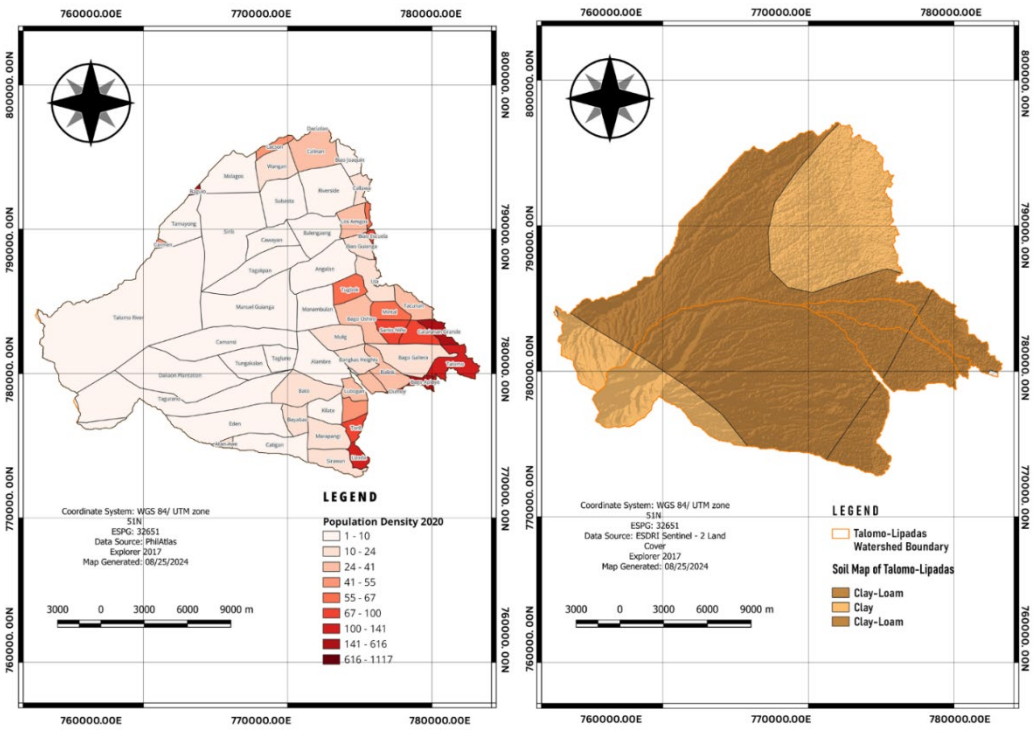

Figure 3. Maps showing population density and soil classification of Talomo-Lipadas Watershed.

In terms of population density as presented in Table 3, data have shown an average population density of 15 person per (ha). The Talomo-Lipadas watershed covers 60 barangays with a total population of 599,066. This implies that the mentioned areas have

large land areas, which are likely to be agricultural and less developed. The low density can also imply less strain on groundwater resources due to low demand for water and fewer impervious surfaces like roads or buildings that prevent water from recharging the aquifers. Although population growth, economic development, and infrastructural, and urban expansions are the main drivers of groundwater fluctuations (Kang et al. 2022). Evidence of large-scale landscape modifications due to the increased human population can change the components of the hydrological cycle such as evapotranspiration, interception, and groundwater recharge (Moeketsi 2022, Mawasha & Britz 2021). The continued expansion of urbanized zones over time could lead to more impervious surfaces and pollution, necessitating integrated water management and land-use planning to maintain groundwater sustainability across the region.

Table 3. Population density of Talomo-Lipadas Watershed.

Total	Barangays	Population	Area (ha)	Population Density
	60	599,066	39595.76	15

Presented in Table 4 is the classification of soil types within the Talomo-Lipadas watershed. Data have shown that 89.06% or a total of 35,240.20 ha and the least is classified as clay-loam with a total land area of 4,355.56 or 10.94% of the total land area. Soil properties and composition can influence how water interacts with the ground, as well as the movement of sediment and nutrient loading in a watershed. Understanding the types of soil within watersheds is key to preventing erosion, managing water flow, and improving water quality which can establish appropriate land management practices to ameliorate water resources. However, clay limits groundwater infiltration and is less permeable. Several studies believe that the blocking effect of clay has an important influence on the formation of groundwater systems (Xing et al. 2018).

Table 4. Soil classification of Talomo-Lipadas Watershed.

Soil Type	Area in (ha)	Area in%
Clay	4355.56	10.94
Clay-Loam	35240.21	89.06
Total	39595.77	100%

Table 5. Buffer Zones Distance Used to Roads and Rivers.

Zone	Distance to Road and River (km)
1	<100
2	100-200
3	200-300
4	300-400
5	400-500

Shown in Table 5 categorizes the ranges of buffer zones utilized in terms of distance to roads and rivers to analyze the proximity of Talomo-Lipadas watershed to water bodies. This table has five (5) zones and each of them represents a specific distance range in kilometers. Zone 1 includes areas within 100 km from roads or rivers, which indicates areas that have been occupied by humans and anthropogenic activities occurred due to

ongoing transportation and distance to water resources. Zone 2 covers distances from 100 to 200 km, which shows areas that are moderately distanced. Zone 3 range is from 200 to 300 km, suggesting areas further distanced from human infrastructure and accessibility of humans starts to decline. Zone 4 spans from 300 to 400 km and shows areas that are in remote or urban regions, where road networks and rivers are long distances. Zone 5, which covers 400 to 500 km, includes isolated and inaccessible areas and has little to no connection to infrastructures.

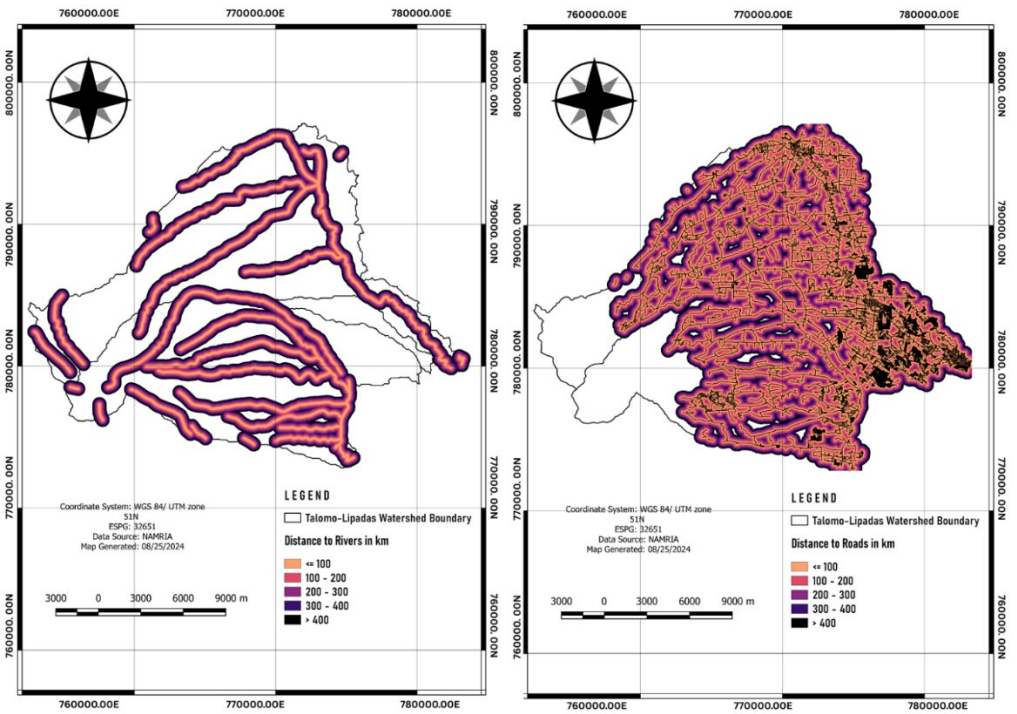

Figure 4. Maps showing the distance to river and distance to road network of Talomo Lipadas Watershed.

For land cover changes, shown in Table 6 is the land use and land cover in the Talomo-Lipadas Watershed in the years 2018-2020. Results revealed that, in 2018, the forest land is the most dominant in the Talomo-Lipadas watershed, starting at 27429.38 ha covering with 69.274% of the total land area, indicating primarily forested landscape which is vital for biodiversity, carbon storage and watershed protection. Followed by built-up areas with 5,960.32 ha comprising 13.50% which reflects a growing urbanization and development, and a considerable portion of the watershed is urbanized. The agricultural accounts the 5,346.17 ha or 13.50%, shrub land with 801.95 ha or 2.03%, grassland with 33.92 ha or 0.09%, water bodies with 23.44 or 0.06% and the least is the bare land with 0.04 ha or 0.001%. This reveals a predominantly rural landscape in the said watershed with significant forest cover highlighting ecological importance of the area while BUA and agricultural activities lands reflect significant human activities. The presence of urban areas indicates growing urbanization pressures, and these changes might alter watershed sediment and solute export (Meybeck & Vorosmarty 2005). Moreover, in 2019 forest lands remain dominant among other land classifications comprising

27,850.94 ha or 70.338% with an increase in its cover of about 70.33%. On the other hand, BUA with 6,448.00 or 16.285% of the total land area with an increase by 16.28% potentially growth in residential, commercial and industrial areas within the watershed, agricultural with 4,371.99 ha or 11.04%, representing with 11.04% down from 15.30% in 2018.

Table 6. Land use and land cover classifications of Talomo-Lipadas Watershed from 2018 to 2020.

LULC Classes	Year								
	2018			2019			2020		
	Area (ha)	%	% (-/+)	Area (ha)	%	% (-/+)	Area (ha)	%	% (-/+)
Built-Up	5960.34	15.053	-	6448.00	16.285	1.23	6834.0	17.2593	0.97
Forest Lands	27463.46	69.360	-	28096.94	70.959	1.60	26480.1	66.88	-4.08
Agricultural	5346.17	13.50	-	4371.99	11.04	-2.46	5599.1	14.14	3.10
Range Lands	801.95	2.03	-	649.66	1.64	-0.38	640.7	1.62	-0.02
Water Bodies	23.44	0.06	-	28.58	0.07	0.01	22.7	0.06	-0.01
Bare Lands	0.41	0.001	-	0.59	0.001	0.00	19.2	0.05	0.05
Total	39595.77	100.000		39595.77	100.000		39595.77	100.0000	

Table 7. Land use and land cover classifications of Talomo-Lipadas Watershed from 2021-2023.

LULC Classes	Year								
	2021			2022			2023		
	Area (ha)	%	% (-/+)	Area (ha)	%	% (-/+)	Area (ha)	%	% (-/+)
Built-Up	7358.21	18.58	1.32	7309.56	18.46	-0.12	7866.58	19.87	1.41
Forest Lands	27452.33	69.33	2.46	27777.65	70.15	0.82	27174.28	68.63	-1.52
Agricultural	4028.34	10.17	-3.97	3916.814	9.89	-0.28	4013.617	10.14	0.24
Range Lands	725.94	1.83	0.22	566.08	1.43	-0.40	516.98	1.31	-0.12
Water Bodies	29.28	0.07	0.02	25.01	0.06	-0.01	24.08	0.06	0.00
Bare Lands	1.67	0.004	-0.04	0.66	0.002	0.00	0.23	0.0006	0.00
Total	39595.77	100.00		39595.77	100.000		39595.77	100.00	

This reduction implies a shift of agricultural use and conversion within this area to other land uses. Shrub land with 649.66 or 1.64% with 1.64%, grassland with 246.00 ha or 0.62% with 0.62%, water bodies with 28.58% or 0.07% slightly increase by 0.07% and bare land with 0.54 ha or 0.001% with 0.001%. Although forest cover has expanded, the countervailing force of other land classification and urban sprawl fueled by suburban growth and improved infrastructure is encroaching on agricultural lands. Furthermore, for the year 2020, forest area is still dominant covering 26199.6 ha or 66.17% with an observed decrease of -2.96%, followed by built-ups by 6834.0 ha or 17.2593% with an increase of 2.99%, agriculture with 5999.1 ha or 14.14% indicating an increase of 14.03%, shrubs with 640.7 ha or 1.62% with an observed decrease of -0.69%, grassland with

280.5 ha or 0.71% with an increase of 7.01%, water bodies covering 22.7 ha or 0.06 shrank by -10.29% and bare lands with 19.3 ha or 0.05% with a large increase in 1737.04%. The expansion of urban areas and increased demand for agricultural land have led to the reduction of forest cover, impacting both quantity and quality of water in the watershed. These changes have altered the hydrological regime, especially in areas where land use and land cover modification influence stream flow patterns (Ebraimian & Nurrudin 2024). As demonstrated in Figure 4, there is an obvious change in the built-up area, and it has been observed that it is increasing over time. In 2021, forest area is still the most extensive land cover type and consistent in terms of the number of hectares accounting for 27205.13 ha or 68.71% although there is a slight increase of 1.92%. On the other hand, urban buildings covered 7358.21 ha or 18.58% with an increase of 3.84%, followed by agricultural land with 4028.344% ha or 10.17% which shrank by -14.03%, shrubs comprising 725. 94 ha or 1.83% with an increase of 6.65%, grassland with 247.20 ha or 0.62 ha with an observed decrease of -5.94, water bodies with 29.28 ha or 0.07 ha with an increase of 14.94%, and lastly, the bare land with 1.67 ha or 0.004% shows a decrease of -45.67%. Although forested areas dominate most of the landscape, experiencing development, especially in the form of urban and agricultural expansion.

The substantial decline in bare land, agriculture, and grassland is an indication of increasing demand for agriculture and development in some forested areas. Recent studies suggested that agriculture and urban settlements at the expense of grassland and bare land mainly due to population decrease and demands for diverse products and soil fertility deterioration (Desalegn et al. 2014). For the year 2022, forest area remained as most dominant land cover with 25274.80 ha or 63.83% marking a decline of -3.55%, followed by agricultural land covering 3916.814 ha or 9.89% showing a decrease of 9.89%, urban built-up with 7309.56 ha or 18.46%, grassland with 2502.85 ha or 6.32% marking a 456.22% rise, shrubland comprising of 566.08 ha or 1.43% reflecting an -11.01% decrease, water bodies with 25.01 ha or 0.06%, a -7.29% reduction, and bare land covering 0.66 ha or 0.002% indicating a -30.24 decrease. This reflects a trend of declining urban, forest, and agricultural areas while an ongoing significant increase in grasslands. Additionally, there seems to be a reduction in water bodies and bare lands. These changes showed a shift in land cover within the watershed. Although the conversion of grassland to agriculture continues, the most significant loss of grassland is due to changing land management coupled with other global change phenomena (Mitchell 2000).

In the year 2023, forest land cover was found consistent throughout the year covering 26395.86 ha or 66.66% marking a 2.22% rise. Whereas agricultural land with 4013.617 ha or 10.14% showing a 1.24% increase, followed by urban built-up comprising 7866.58 ha or 19.87% reflecting a 19.87% growth, grassland with 778.42 ha or 1.97% a -32.58% decrease, shrubs with 516.98 ha or 1.31% a -4.34% decline, water bodies covering 24.08 ha or 0.06% a dropped by -1.86%, and lastly the bare land with 0.32 ha or 0.0006% a -32.58 drop. Population pressure, agricultural expansion, and policy and tenure insecurity were the major driving forces behind the land use and land cover change altering some hydrologic processes (Gaur et al. 2021). The changes were driven by proximate and underlying drivers and these main drivers are the expansion of agricultural activities, urban and infrastructure expansion, and demographic factors. Consequently, the natural resource base of the watershed is degrading (Anteneh et al. 2018). Moreover, several studies suggested that unmanaged conversion of land cover was affecting the natural vegetation base and hydrology in watersheds. Thus, integrated watershed planning, and management have paramount importance in maintaining economic and ecological benefits (Degife et al. 2019).

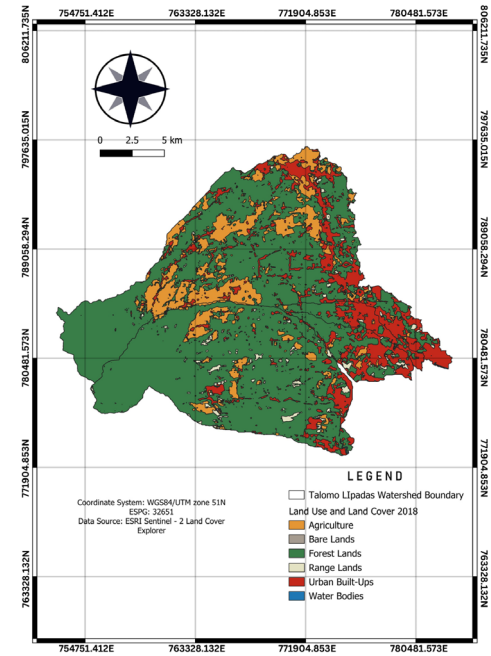
754751.412E
763328.132E
771904.853E
780481.573E
806211.735N
797635.015N
789058.294N
780481.573N
771904.853N
763328.132N
0 2.5 5 km
LEGEND
Coordinate System: WGS84/UTM zone 51N
ESPG: 32651
Data Source: ESRI Sentinel - 2 Land Cover Explorer
Talomo LIpadas Watershed Boundary
Land Use and Land Cover 2018
Agriculture
Bare Lands
Forest Lands
Range Lands
Urban Built-Ups
Water Bodies

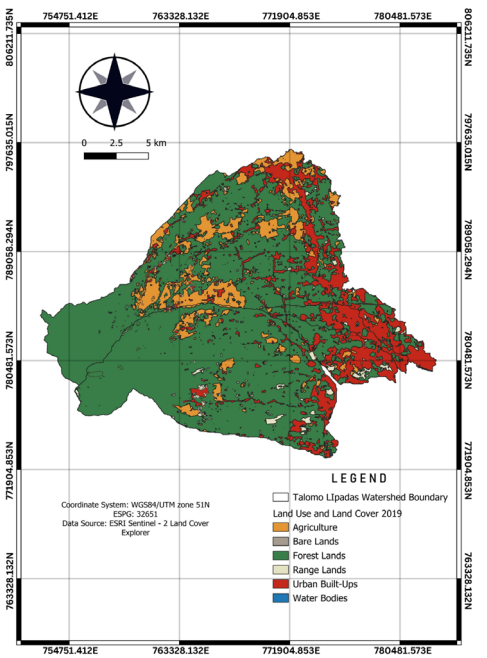
754751.412E
763328.132E
771904.853E
780481.573E
806211.735N
797635.015N
789058.294N
780481.573N
771904.853N
763328.132N
0 2.5 5 km
LEGEND
Coordinate System: WGS84/UTM zone 51N
ESPG: 32651
Data Source: ESRI Sentinel - 2 Land Cover Explorer
Talomo LIpadas Watershed Boundary
Land Use and Land Cover 2019
Agriculture
Bare Lands
Forest Lands
Range Lands
Urban Built-Ups
Water Bodies

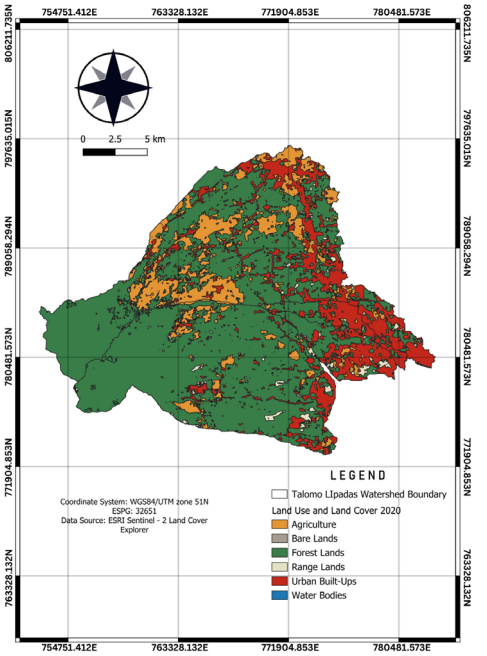
754751.412E
763328.132E
771904.853E
780481.573E
806211.735N
797635.015N
789058.294N
780481.573N
771904.853N
763328.132N
0 2.5 5 km
LEGEND
Coordinate System: WGS84/UTM zone 51N
ESPG: 32651
Data Source: ESRI Sentinel - 2 Land Cover Explorer
Talomo LIpadas Watershed Boundary
Land Use and Land Cover 2020
Agriculture
Bare Lands
Forest Lands
Range Lands
Urban Built-Ups
Water Bodies

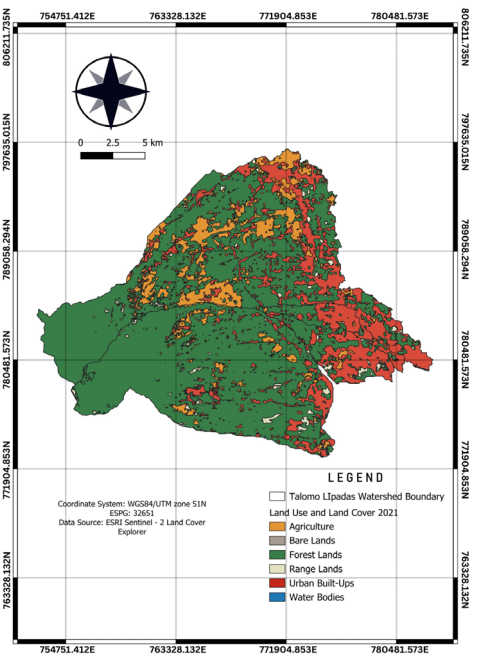
754751.412E
763328.132E
771904.853E
780481.573E
806211.735N
797635.015N
789058.294N
780481.573N
771904.853N
763328.132N
0 2.5 5 km
LEGEND
Coordinate System: WGS84/UTM zone 51N
ESPG: 32651
Data Source: ESRI Sentinel - 2 Land Cover Explorer
Talomo LIpadas Watershed Boundary
Land Use and Land Cover 2021
Agriculture
Bare Lands
Forest Lands
Range Lands
Urban Built-Ups
Water Bodies

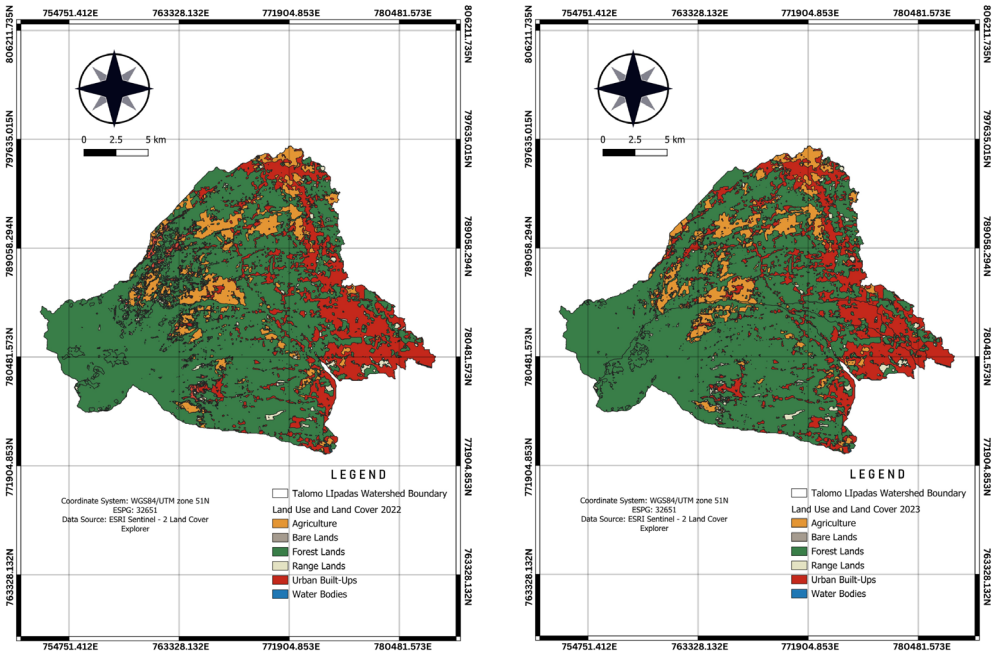

Figure 5. Land use and land cover changes of Talomo-Lipadas Watershed from 2018 to 2023.

Figure 6 have shown the trend of rainfall patterns in Talomo-Lipadas watershed from 2018-2023. Also, shown in the map on rainfall distribution in Talomo-Lipadas watershed. Its spatial distribution is presented in the map in Figure 7. Moreover, the rainfall received in the past years is above the threshold trend indicating groundwater recharge. However, in 2023 it declines of approximately 300 mm indicating lower rainfall receive throughout the year implying lower groundwater recharge. On the other hand, the amount of surface runoff and water recharge caused by rainfall is strongly dependent on rainfall intensity, and the interactions between them have been examined in depth (Wang et al. 2015). It shows that the rainfall distribution from 2018-2020 gradually changes. In 2018, the rainfall distribution was at its highest in the southern and southeastern areas of the watershed with greater than 68.6 mm rainfall, while the lowest was in the northern areas of the watershed with less than or equal to 57.7 mm rainfall. In 2019, the rainfall distribution is at its highest in the northern areas of the watershed with greater than 116.6 mm rainfall, while the lowest is in the eastern part of the watershed with less than or equal to 34.8 mm rainfall.

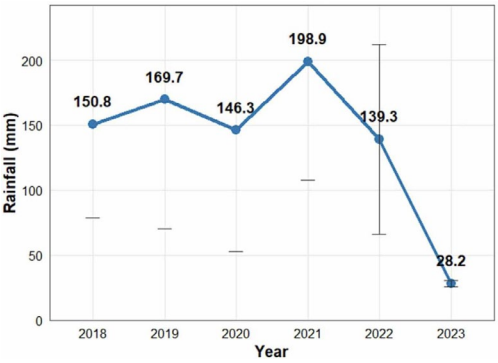

Figure 6. Graph showing rainfall trends of Talomo-Lipadas Watershed from 2018 to 2023.

In 2020, the rainfall distribution is at its highest in the southwestern, southern, and southeastern areas of the watershed with greater than 53.7 mm rainfall, while the lowest

is in the northern and eastern parts of the watershed with less than or equal to 33.1 mm rainfall. In 2021, the rainfall distribution is at its highest in the southwestern, southern, and southeastern areas of the watershed with greater than 53.7 mm rainfall, while the lowest is in the northern and eastern parts of the watershed with less than or equal to 33.1 mm rainfall, same with 2020. In 2022, the rainfall distribution is at its highest in the eastern areas of the watershed with 141.0 mm rainfall, while the lowest is in the northern areas of the watershed with less than or equal to 93.5 mm rainfall. In 2023, the rainfall distribution is at its highest in the northern areas of the watershed with 28.7 mm rainfall, while the lowest is in the eastern areas of the watershed with 27.9 mm rainfall significantly impacts groundwater recharge, which affects runoff processes (Zheng et al. 2023).

Groundwater Availability Projection

Presented in Table 8 is the projected groundwater level in Talomo-Lipadas watershed using various statistical models. The supply value of 280.5 mld is the capped or baseline value for available water. DCWD columns show the actual figures, and the three models were performed to forecast the missing values from the year 2018 to 2023. It shows that there is a gradual increase from 134.61 mld to 357.84 mld in 2017. The linear model shows a steady rise in water demand, ranging from 121.2 in 1997 to 410.99 in 2023. This model suggests a straightforward and consistent rate of increase. The exponential model, on the other hand, projected sharper and larger values in demand over time. For instance, the figure predicted in 2019 is 389.34 mld and it abruptly jumps to 544.92 in 2023. This indicates a possible growth in water demand due to the continuous urban expansion and population. Lastly, the cubic model is more complex and reflects fluctuations in the growth rate. Compared to the other two models, cubic provided lower estimates in the early years and had a moderate growth curve in the later years. Another instance is in 2018, the projected value is 372.69 mld and as the years pass by, it gradually increases but not that sharp by almost 470 mld. These models could serve as vital tools for future planning, especially in calculating potential demand pressures on the water supply system.

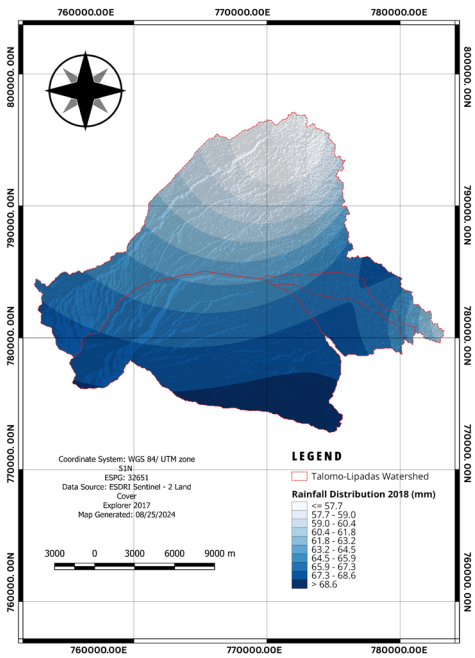

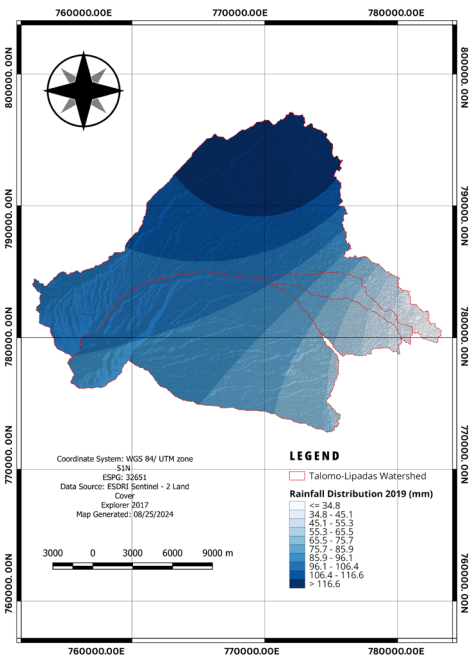

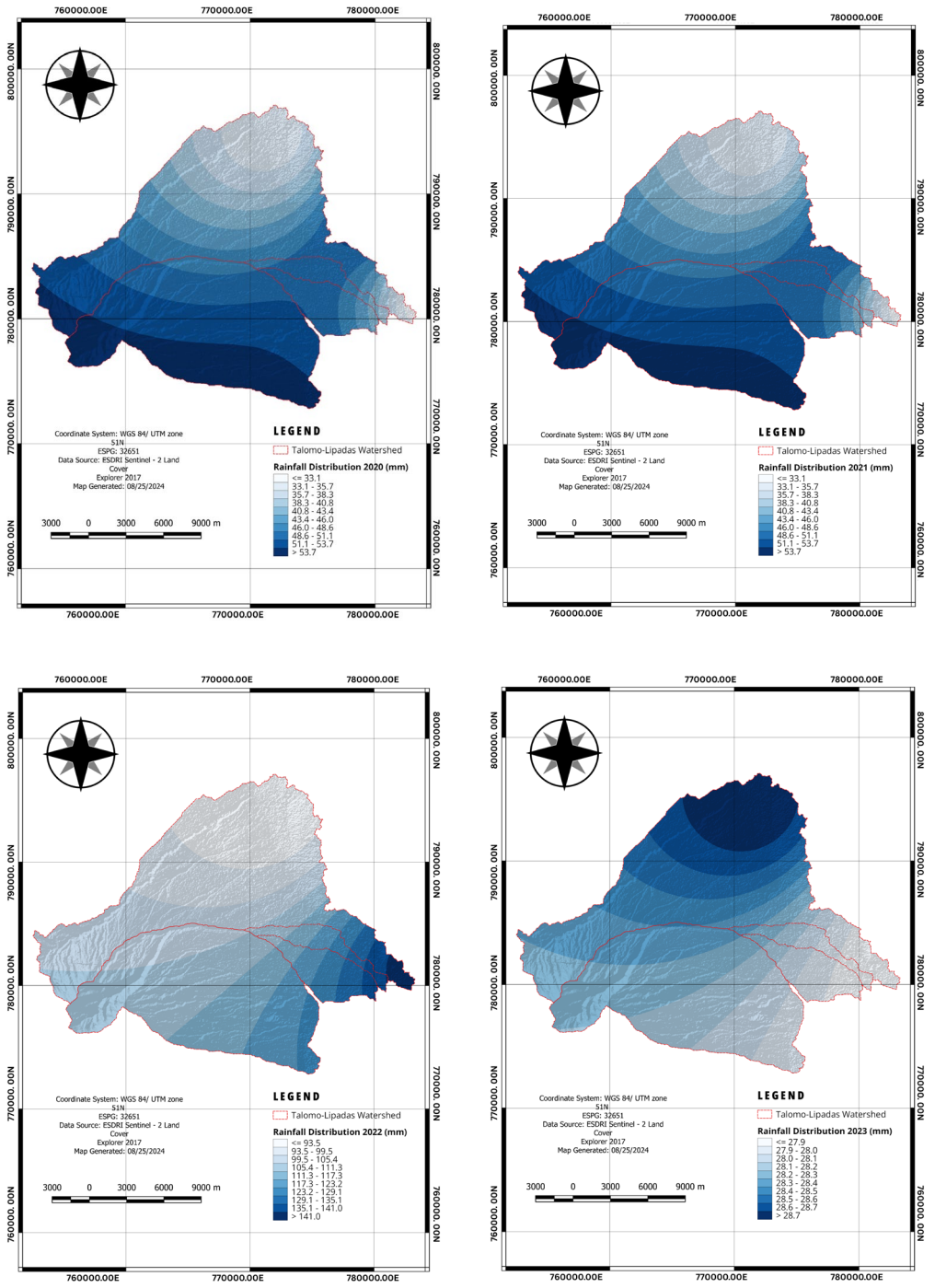

Figure 7. Maps showing the rainfall distribution of Talomo-Lipadas Watershed from 2018 to 2023.

Table 8. Projected Groundwater Levels from Talomo-Lipadas Watershed in Million Liters per Day (mld), where - no data. After Espina (2022).

Year	Water Supply	DCWD	Linear Model	Exponential Model	Cubic Model
1997	280.5	134.61	121.2	134.58	134.94
2001	280.5	163.68	165.72	163.25	162.47
2005	280.5	199.03	210.24	198.03	200.07
2009	280.5	242.03	254.76	240.23	246.16
2011	280.5	280.5	277.02	264.59	271.89
2013	280.5	294.32	299.28	291.41	299.15
2017	280.5	357.87	343.8	353.5	357.46
2018	280.5	-	354.93	370.99	238.87
2019	280.5	-	366.06	389.34	243.50
2020	280.5	-	377.19	408.6	403.75
2021	280.5	-	388.73	494.75	430.82
2022	280.5	-	399.86	519.23	448.53
2023	280.5	-	410.99	544.92	466.70

Figure 8 provides visual presentations to compare the behavior of the three models. The linear model shows a steady rise in demand, since the growth rate is constant, the model assumes a fixed rate annually and this is useful when future demands are increasing without pressure or acceleration. The exponential model projects rapid and sharp growth. This means that it is more accelerated than the linear model. Cubic accounts for fluctuations. The curve on the graph is not as steep as the exponential model but it demonstrates a gradual upward trend. Overall, the figures calculated by the three models are increasing annually and offer a comprehensive view of future water supply but with slight differences in the behavior of the growth rate.

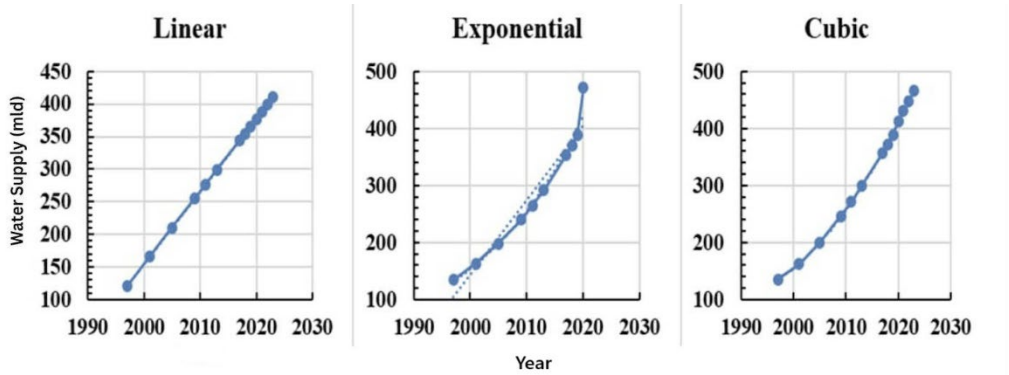

Figure 8. The statistical models in projecting the groundwater supply in Talomo-Lipadas Watershed (without the predictors).

Table 9. Projected Groundwater Levels from Talomo-Lipadas Watershed in million liters per day (mld). Bold fonts - forecasted, regular fonts - based from Espina (2022).

Year	Water Supply	DCWD	Linear Model	Exponential Model	Cubic Model	SVR
1997	280.5	134.61	121.2	134.58	134.94	141.01
2001	280.5	163.68	165.72	163.25	162.47	162.49
2005	280.5	199.03	210.24	198.03	200.07	202.74
2009	280.5	242.03	254.76	240.23	246.16	247.72
2011	280.5	280.5	277.02	264.59	271.89	274.08
2013	280.5	294.32	299.28	291.41	299.15	300.75
2017	280.5	357.87	343.8	353.5	357.46	325.09
2018	280.5	-	354.93	370.99	372.69	313.59
2019	280.5	-	366.06	389.34	388.13	301.86
2020	280.5	-	377.19	408.6	403.75	310.73
2021	280.5	-	388.73	494.75	430.82	243.94
2022	280.5	-	399.86	519.23	448.53	294.76
2023	280.5	-	410.99	544.92	466.70	236.31

Figure 9 illustrates the projected groundwater availability from 1997 to 2023, factoring in the influence of Land Use Land Cover (LULC) change, particularly in urban built ups expansion percentage and rainfall data. From 1997 to 2017, the graph shows a consistent upward direction in groundwater levels, reflecting increasing availability. This rise likely corresponds to precipitation patterns, land use dynamics, and population, which contribute to progressive groundwater recharge. The peak in groundwater levels occurred around 2017-2018, marking the period of highest projected availability. However, following this peak, the trend projection shows a marked decline from 2018 onwards. This decreases in groundwater levels from 2019 to 2023 suggests that the combination of changing LULC, such as urban expansion, deforestation, or agricultural practices, and shifts in precipitation patterns may negatively impact groundwater replenishment (Adeleke et al. 2015). Based on the findings under land use land cover change data, 25% of the prior dominant land cover of the watershed, forest covers were converted to urban build ups. This noticeable change is reflected in the model, which indicates a decreasing trend from 357.87 mld in 2017 (highest peak) to 236.31 mld in 2023 (lowest), and is particularly concerning for future water resource management (Mandal 2024), as it suggests potential challenges in maintaining sustainable groundwater supplies under current land use and rapid change in climatic conditions. The use of SVR from 2018 to 2023 provides a more informed projection, but the declining trend should be monitored as there is a need for immediate action to mitigate future water scarcity risks. Furthermore, extensive monitoring and recording of groundwater levels in the Davao City, especially in cities with insufficient tools, is crucial for further validating these projections which can be helpful in developing responsive water management strategies.

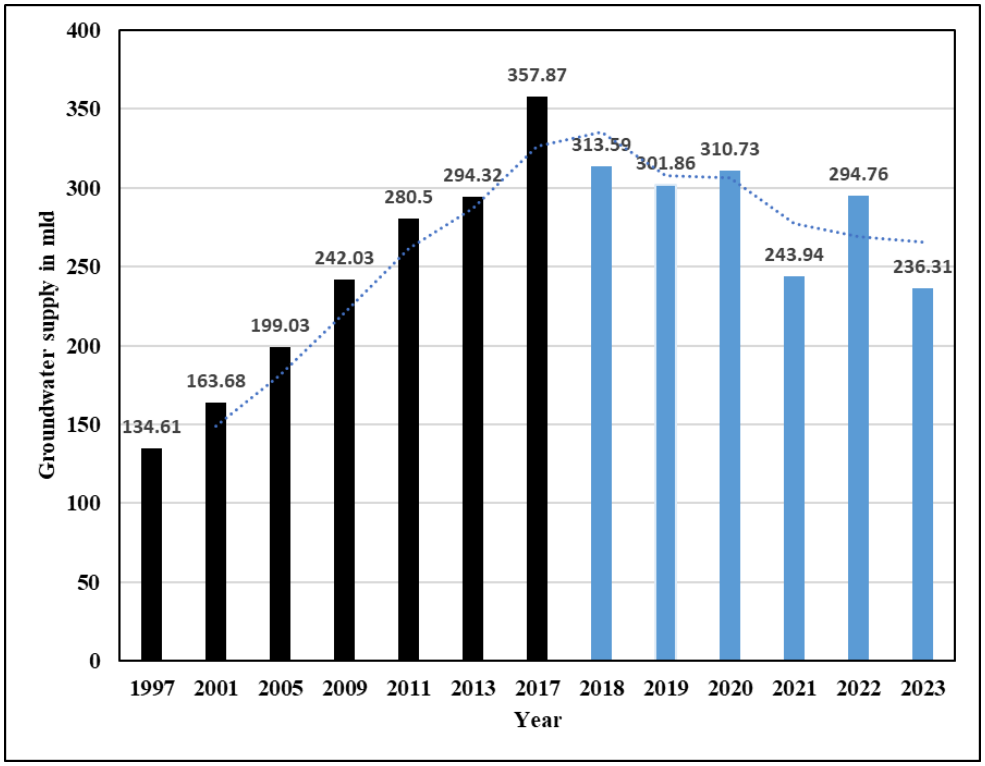

Figure 9. Projected groundwater availability based on LULC change (urbanization) and precipitation changes using Support Vector Regression from 2018 to 2023.

Table 10 presents the R-squared values for four projection models, which measure how each model fits the observed data. The Exponential Model has an R-squared value of 0.87, indicating a reasonably good fit, although it has unexplained variations. This model captures rapid growth but may not account for all the nuances in the data. The Cubic Model has a higher R-squared value of 0.90, suggesting it provides a better fit by incorporating more complex and handling non-linear trends more effectively. The Linear Model shows an R-squared value of 0.88, indicating that it also performs well, though it is slightly less accurate than the cubic model. The linear model's assumption of a constant growth rate works well but may oversimplify the actual trends. Lastly, the Support Vector Regression Model has the highest R-squared value of 0.93, indicating it is the most accurate among all models in explaining the variance in the data. This model's superior performance likely results from its ability to incorporate multiple influencing factors, such as land use changes and precipitation dynamics, into its projections (Khalifeloo et al. 2015). Overall, while all models show strong predictive ability with R-squared values above 0.87, the Support Vector Regression model emerges as one of the most reliable for forecasting groundwater levels together with convolutional neural network (Panahi et al. 2020), followed by the cubic, linear, and exponential models. This highlights the importance of using comprehensive approaches that factor in various dynamics for more precise predictions.

Table 10. R-squared values of 4 projection models of groundwater availability.

Projection Models	Computed R-squared
Exponential	0.87
Cubic	0.90
Linear	0.88
Support Vector Regression Model	0.93

Table 10 shows the regression statistics for the relationship between Land Use Land Cover Change (LULCC) and Projected Groundwater Availability, are used to reveal how LULCC influences groundwater levels. The Multiple R-values of 0.92 indicate a strong positive correlation (Ramirez et al. 2022), suggesting that changes in land use are closely tied to variations in groundwater availability. The R-squared value of 0.80 shows that 80% of the variance in projected groundwater levels can be explained and affected by LULC changes, signifying a robust model fit. The Adjusted R-squared value of 0.85 further strengthens this interpretation, indicating that the model remains highly accurate even after accounting for additional factors. The Standard Error of 0.20 implies that the predicted values deviate only slightly from the actual observations, which supports the accuracy of the model. The F-statistic of 6.35 confirms that the overall regression model is statistically significant, meaning that LULC has a strong impact on groundwater availability. The p-value of 0.015 reinforces this, indicating that the likelihood of this relationship being due to random chance is very low. The regression analysis demonstrates a strong and statistically significant relationship between LULC and projected groundwater availability. This suggests that changes in land use play a crucial role and have a direct impact in influencing groundwater levels (Goswami et al. 2024), making it an important consideration for water resource management and planning.

Table 11. Regression statistics of land use land cover and projected groundwater availability.

Regression Statistics	
Multiple R	0.92
R Square	0.80
Adjusted R Square	0.85
Standard Error	0.20
F – statistic	6.35
p-value (F – statistic)	0.02

CONCLUSIONS

Findings of the study in the Talomo-Lipadas watershed that majority of the land area falls under the slope gradient ranges from 15-30% classified as rolling to moderate covering 85% of the total land area comprises the 33,651.97 ha and the least is classified as very steep ranges 50% and above which accounts the 5.01% of the total land area with 1,981.74 ha. The elevation gradient ranges from <530 m a.s.l. with 89.79% and the least elevation gradient is 2,139-2,673 ma.s.l. with .05% and population density of 15 km^2. Dominant soil classification is clay-loam with 89.06% and the least is clay with 10.94%, buffer areas categorized into five zones with an interval of <100km. Land use and land cove changes, in terms of land LULC changes, the highest in BUA is in 2019 with 1.41%, forest land experiences decline with largest in 2020 with -4.08%. The agricultural classification is in declining trend with highest in 2021 with -3.97%, shrub land with highest decline in 2022 with -.40%. On the other hand, waterbodies are on an increasing trend with significant increase in 2021 with +.02, bare lands with +.66 in 2021. Precipitation patterns have

shown downward trends in the last five in which year 2023 had accumulated the lowest amount of rainfall in mm approximately more than 300 mm. In predicting groundwater availability, four (4) models can predict groundwater availability showing varied characteristics and implies increasing availability in groundwater excluding predictors. Moreover, the projected groundwater availability in the Talomo-Lipadas watershed has shown downward form year 2018 considering LULC changes and precipitation ranges as predictor variables. Also, four (4) projection models were tested and were confirmed as best fit models that predict groundwater availability with computed R^2 for exponential-.87, cubic-.90, linear-.88 and SVR-.93. Regression statistics confirmed land use and land cover changes and precipitation ranges with an adjusted R^2 of .85 indicating correlation and strong impact between groundwater availability and the predictor variables significant at .05 confidence interval.

ACKNOWLEDGEMENTS

First, the researchers would like to extend gratitude to the University of Mindanao for providing invaluable guidance necessary to complete this study. The conducive academic environment and support of the faculty of Environmental Studies Department have helped the researchers throughout this journey. We would also like to thank our research adviser, Dr. Jason Ben Paragamac for his hands-on approach in shaping the direction and quality of this research. His expertise and mentorship have been instrumental in making excellent outcome of this work. We also want to extend my heartfelt thanks to For. Rylle Anuber for his assistance in the generation of critical maps and geospatial data. To the whole group for their unwavering commitment and teamwork. The collaboration and shared efforts that has put into this project made this study not only possible but also a rewarding and enriching experience. The dedication, patience, and motivation of the entire research team were key to achieving our goals.

REFERENCES

Adeleke O.O., Makinde V., Eruola A. O., Dada O.F., Ojo A.O., Aluko T.J. 2015. Estimation of groundwater recharge in Odeda Local Government Area, Ogun State, Nigeria using Empirical Formulae. *Challenges* 6(2): 271-281. https://doi.org/10.3390/challe6020271

Aldridge C., Baker B. 2017. Watersheds: role, importance, & stewardship. *Water-shed: Role, Importance, & Stewardship*. http://extension.msstate.edu/publications/watersheds-role-impotance-stewardship. [Accessed in 10.09.2024].

Anteneh Y., Stellmacher T., Zeleke G., Mekuria W., Gebremariam E. 2018. Dynamics of land change: insights from a three-level intensity analysis of the Legedadie-Dire catchments, Ethiopia *Environmental monitoring and assessment* 190(5): 309. https://doi.org/10.1007/s10661-018-6688-1

ArcGIS Living Atlas of the World. n.d. GIS Content from the Geospatial Community. https://www.esri.com/en-us/arcgis/products/living-atlas. [Accessed in 05.09.2024].

Banjara M., Bhusai A., Ghimire A.B., Kalra A. 2024. Impact of Land Use and Land Cover Change on Hydrological Processes in Urban Watershed: Analysis and Forecasting for Flood Risk Management. *Geoscience* 14(2): 40. https://doi.org/10.3390/geosciences14020040

Barrett J.P. 1974. The Coefficient of Determination—Some Limitations. *The American Statistician* 28(1): 19–20. https://doi.org/10.1080/00031305.1974.10479056

Bieger K., Arnold J.G., Rathjens H., White M.J., Bosch D.D., Allen P.M., Volk M.,

Srinivasan R. 2016. Introduction to<scp>SWAT</scp>+, a completely restructured version of the soil and water assessment tool. *JAWRA Journal of the American Water Resources Association* 53(1): 115–130. https://doi.org/10.1111/1752-1688.12482.

Branzuela N.E., Faderogao F.J.F., Pulhin J.M. 2015. Downscaled Projected Climate Scenario of Talomo-Lipadas Watershed, Davao City, *Philippines. Journal of Earth Science & Climatic Change* 6(3): 1. https://www.omicsonline.org/open-access/downscaled-projected-climate-scenario-of-talomolipadas-watersheddavao-city-philippines-2157-7617-1000268.php?aid=41767. [Accessed in 10.09.2024].

Dai X., Xie Y., Simmons C.T., Berg S., Dong Y., Yang J., Love A.J., Wang C., Wu J. 2021. Understanding topography-driven groundwater flow using fully coupled surface-water and groundwater modeling, *Journal of Hydrology* 594: 125950. https://doi.org/10.1016/j.jhydrol.2020.125950

Desalegn T., Cruz-Souza F., Kindu M., Turrion M.B. 2014. Land-use/land-cover (LULC) change and socioeconomic conditions of the local community in the central highlands of Ethiopia. *International Journal of Sustainable Development & World Ecology* 21(5): 406–413. https://doi.org/10.1080/13504509.2014.961181

Degife A., Worku H., Gizaw S., Legesse A. 2019. Land use land cover dynamics, its drivers and environmental implications in Lake Hawassa Watershed of Ethiopia. *Remote Sensing Application: Society and Environment* 14: 178–190. https://doi.org/10.1016/j.rsase.2019.03.005

Ebrahimian M., Nurruddin A.A. 2024. Quantitative assessment of past and future tropical forest transition and its dynamic to streamflow of catchment, Malaysia. *IForest-Biogeosciences and Forestry* 17(3): 181–19. https://doi.org/10.3832/ifor4339-017

Espina R. U. 2013. The Water-Energy Nexus: Exploring Options for Davao's Future. *TAMBARA*, *30*(1): 43–60. https://www.researchgate.net/publication/359866729_The_Water-Energy_Nexus_Exploring_Options_for_Davao's_Future. [Accessed in 09.10.2024].

Fao/UNESCO soil map of the world. Fao soils Portal. Food and agriculture organization of the United Nations. 1961. https://www.fao.org/soils-portal/data-hub/soil-maps-and-databases/faounesco-soil-map-of-the-world/en/. [Accessed in 13.09.2024].

Gaur S., Bandyopadhyay A., Singh R. 2021. Projecting land use growth and associated impacts on hydrological balance through scenario-based modelling in the Subarnarekha basin, India. *Hydrological Sciences Journal* 66(14): 1997–2010. https://doi.org/10.1080/02626667.2021.1976408

Goswami G., Darang J., Prasad R.K., Mandal S. 2024. Evaluating water availability and flow characteristics for Dikrong River in Arunachal Pradesh using Acoustic Doppler Current Profiler. *Sustainable Water Resources Management* 10(103). https://doi.org/10.1007/s40899-024-01082-7

Grinevskii S.O. 2014. The effect of topography on the formation of groundwater recharge. *Moscow University Geology Bulletin* 69: 47–52. https://doi.org/10.3103/S0145875214010025, 2014

Ibañez J., Tampos G., Maglinte P., Reazonda M., Villanueva A., Bañes A. 2012. Panigan Tamugan and Talomo-Lipadas Watersheds Resource and Socio-Economic Assessment (RSEA) Final Technical Report. 2012. https://idisphil.org/wp-content/uploads/2019/03/Talomo_Lipadas_and_Panigan_Tamugan_RSEA_2013-FINAL-TECHNICAL-REPORT.pdf [Accessed in 13.09.2024].

Kang J., Wang Z., Cheng H., Wang J., Lui X. 2022. Remote sensing land use evolution in earthquake-stricken regions of Wenchuan county, China. *Sustainability* 14(15): 9721. https://doi.org/10.3390/ su14159721

Khalifeloo M.H., Mohammad M., Heydari M. 2015. Multiple imputations for hydrological missing data by using a regression method (Klang River Basin). *International Journal of Research in Engineering and Technology* 4,519–524.https://www.researchgate.net/profile/Mohammad-Heydari-13/publication/280133803_MULTIPLE_IMPUTATION_FOR_HYDROLOGICAL_MISSING_DATA_BY_USING_A_REGRESSION_METHOD_KLANG_RIVER_BASIN/links/55ac0d5b08aea994672799aa/MULTIPLE-IMPUTATION-FOR-HYDROLOGICAL-MISSING-DATA-BY-USING-A-REGRESSION-METHOD-KLANG-RIVER-BASIN.pdf. [Accessed in 11.09.2024].

Kowalczyk A. 2014. *Support vector regression with R*. SVM Tutorial. www.svm-tutorial.com/2014/10/support-vector-regression-r/. [Accessed in 08.07.2025].

Mandal B. 2024. Leveraging Machine Learning for Analyzing the Nexus Between Land Use and Land Cover Change, Land Surface Temperature and Biophysical Indices in an Eco-Sensitive Region of Brahmani-Dwarka Interfluve. *Results in Engineering* 24: 102854. https://doi.org/10.1016/j.rineng.2024.102854

Mawasha T., Britz W. 2021. Hydrological Impacts of Land Use-Land Cover Change on Urban Flood Hazard: A Case Study of Jukskei River in Alexandra Township, Johannesburg, South Africa. *South African Journal of Geomatics* 10(2). https://www.ajol.info/index.php/sajg/article/view/231210. [Accessed in 22.09.2024].

Meybeck M., Vörösmarty C. 2005. Fluvial filtering of land-to-ocean fluxes: from natural Holocene variations to Anthropocene. *Comptes Rendus Geoscience* 337(1-2): 107–123. https://doi.org/10.1016/j.crte.2004.09.016

Meyer D., Dimitriadou E., Hornik K., Weingessel A., Leisch, F. 2024. _e1071: Misc Functions of the Department of Statistics, Probability Theory Group (Formerly: E1071), TU Wien_. R package version 1.7-16. https://CRAN.R-project.org/package=e1071. [Accessed in 10.10.2024].

Mitchell J.E. 2000. Rangeland Resource Trends in the United States. Fort Collins (CO): *USDA Forest Service Rocky Mountain Research Station. General Technical Report RMRS-GTR-68*. https://www.fs.usda.gov/rm/pubs/rmrs_gtr068.pdf. [Accessed in 22.09.2024].

Moeketsi P., Nkhonjera G., Alowo R. 2022. Changes in land use land cover within the Jukskei River basin and its implications on the water availability. *IOP Conference Series Earth and Environmental Science* 1087(1): 012035. https://doi.org/10.1088/1755-1315/1087/1/012035

Montoya S. 2017. Learn about QSWAT, the hydrological model SWAT in QGIS - Hatari Labs. Hatari Labs. https://hatarilabs.com/ih-en/learn-about-qswat-the-hydrological-model-swat-in-qgis. [Accessed in 21.09.2024].

Morbidelli R., Saltalippi C., Flammini A., Govindaraju R.S. 2018. Role of slope on infiltration: a review. *Journal of Hydrology*, *557*: 878-886. https://doi.org/10.1016/j.jhydrol.2018.01.019

Mukherjee A., Ramachandran P. 2018. Prediction of GWL with the help of GRACE TWS for unevenly spaced time series data in India: analysis of comparative performances of SVR, ANN and LRM. *Journal of hydrology* 558: 647–658. https://doi.org/10.1016/j.jhydrol.2018.02.005

NASA Shuttle Radar Topography Mission (SRTM). 2013. Shuttle Radar Topography Mission (SRTM) Global. Distributed by

OpenTopography. https://doi.org/10.5069/G9445JDF. [Accessed 2025.07.31].

OpenStreetMap Downloader Plugin (OSM). 2015. OSMDownloader. https://plugins.qgis.org/plugins/OSMDownloader/. [Accessed in 22.10.2024].

Pepin N., Arnone E., Gobiet A., Haslinger K., Kotlarski S., Notarnicola C., Palazzi E., Seibert P., Serafin S., Schoner W., Terzago S., Thornton, M., Vuille, M., Adler, C. 2022. Climate change and their elevation patterns in the Mountains of the World. *Review of Geophysics* 60: 1. https://doi.org/10.1029/2020RG000730

PhilAtlas Website. 2024. PhilAtlas. https://www.philatlas.com/. [Accessed in 10.22.2024].

Ramirez S.G., Williams G.P., Jones N.L. 2022. Groundwater level data imputation using machine learning and remote earth observations using inductive bias. *Remote Sensing* 14(21): 5509. https://doi.org/10.3390/rs14215509

Roumasset J., Wada C.A. 2013. A dynamic approach to PES pricing and finance for interlinked ecosystem services: Watershed conservation and groundwater management. *Ecological Economics* 87: 24–33. https://doi.org/10.1016/j.ecolecon.2012.11.023

Satapathy D.P., Sahoo S.K. 2023. Prediction of ground water level using SVM-WOA approach: A case study. *Journal of Scientific & Industrial Research* 82: 269–277. https://doi.org/10.56042/jsir.v82i2.70212

Panahi M., Sadhasivam N., Pourghasemi H.R., Rezaie F., Lee S. 2020. Spatial prediction of groundwater potential mapping based on convolutional neural network (CNN) and support vector regression (SVR). *Journal of Hydrology* 588: 125033. https://doi.org/10.1016/j.jhydrol.2020.125033

Sertel E., Imamoglu M.Z., Cuceloglu G., Erturk A. 2019. Impacts of land cover/use changes on hydrological processes in a rapidly urbanizing mid-latitude water supply catchment. *Water* 11(5): 1075. https://doi.org/10.3390/w11051075

Simlandy S. 2015. Importance of Groundwater as Compatible with the Environment. *International Journal of Ecosystem* 5(3A): 89–92. http://article.sapub.org/10.5923.c.ije.201501.13.html. [Accessed in 21.09.2024].

Sun G., Caldwell P.V. 2015. Impacts of urbanization on stream water quantity and quality in the United States. *Water Resources Impact* 17(1): 4. https://research.fs.usda.gov/treesearch/47460. [Accessed in 21.09.2024].

Wang H., Gao J.E., Zhang M., Li X., Zhang S., Jia, L. 2015. Effects of rainfall intensity on groundwater recharge based on simulated rainfall experiments and a groundwater flow model. *CATENA* 127: 80–91. https://doi.org/10.1016/j.catena.2014.12.014

Xing L., Huang L., Yang Y., Xu J., Zhang W., Chi G., Hou X. 2018. The blocking effect of clay in groundwater system: a case study in an inland plain area. 15(9): 1816. https://doi.org/10.3390/ijerph15091816

Yuan C., Weng Y., Xiong K., Rong L. 2024. Projections of land use change and water supply–demand assessment based on climate change and socioeconomic scenarios: a case study of Guizhou Province, China. *Land* 13(2): 194. https://doi.org/10.3390/land13020194

Zheng W., Wang S., Tan K., Shen Y., Yang L. 2023. Rainfall intensity affects the recharge mechanisms of groundwater in a headwater basin of the North China Plain. *Applied Geochemistry* 155: 105742. https://doi.org/10.1016/j.apgeochem.2023.105742

Received:30.10.2024.
Accepted: 30.07.2025.